Microchim Acta (2013) 180:767–774
DOI 10.1007/s00604-013-0985-8

ORIGINAL PAPER

Label-free electrochemical immunosensor for the carcinoembryonic antigen using a glassy carbon electrode modified with electrodeposited Prussian Blue, a graphene and carbon nanotube assembly and an antibody immobilized on gold nanoparticles

Dexiang Feng · Xiaocui Lu · Xiao Dong · Yunyun Ling · Yuzhong Zhang

Received: 25 January 2013 / Accepted: 21 March 2013 / Published online: 6 April 2013

Abstract We described a sensitive, label-free electrochemical immunosensor for the detection of carcinoembryonic antigen. It is based on the use of a glassy carbon electrode (GCE) modified with a multi-layer films made from Prussian Blue (PB), graphene and carbon nanotubes by electrodeposition and assembling techniques. Gold nanoparticles were electrostatically absorbed on the surface of the film and used for the immobilization of antibody, while PB acts as signaling molecule. The stepwise assembly process was investigated by differential pulse voltammetry and scanning electron microscopy. It is found that the formation of antibody-antigen complexes partially inhibits the electron transfer of PB and decreased its peak current. Under the optimal conditions, the decrease of intensity of the peak current of PB is linearly related to the concentration of carcinoembryonic antigen in two ranges (0.2–1.0, and 1.0–40.0 ng·mL^{-1}), with a detection limit of 60 pg·mL^{-1} (S/N=3). The immunosensor was applied to analyze five clinical samples, and the results obtained were in agreement with clinical data. In addition, the immunosensor exhibited good precision, acceptable stability and reproducibility.

Keywords Immunosensor · Carcinoembryonic antigen · Graphene · Prussian blue · Carbon nanotubes · Gold nanoparticles

Introduction

Tumor markers are substances existing in tumor cells or host body fluids, which are produced by tumors associated with cancers. The elevation of tumor markers in human serum is related to patients with certain types of cancer. Carcinoembryonic antigen (CEA) is one of the most important tumor markers in clinical diagnosis. For healthy individuals, the levels of CEA in serum are low than 5 ng·mL^{-1}, if the level of CEA in serum is higher than the value, it is possible to arouse colon cancer and breast cancer or other cancers [1, 2] and so on. Thus, it is effective helps for early tumors diagnoses and treatment of cancer to monitor the changes of the CEA concentration in serum. Hence, searching for a sensitive, rapid, simple method for the CEA detection would be of great interest in clinical diagnosis.

Immunoassay based on the antibody-antigen interaction is one of the most important analytical techniques in the quantitative detection of tumor markers. To date, many kinds of immunoassay techniques have been reported including as enzyme-linked immunosorbent [3], surface-plasmon resonance [4], chemiluminescence [5] and electrochemistry [6]. Among these methods, electrochemical immunoassay techniques have attracted considerable interests because of their simplicity, high sensitivity, selectivity and low cost. Recently, some electrochemical immunosensors have been reported for the determination of tumor markers [7–11]. Most of the electrochemical immunosensors are performed depend on the

Electronic supplementary material The online version of this article (doi:10.1007/s00604-013-0985-8) contains supplementary material, which is available to authorized users.

D. Feng · X. Lu · X. Dong · Y. Zhang (✉)
College of Chemistry and Materials Science, Anhui Key Laboratory of Chemo-Biosensing, Anhui Normal University, Wuhu 241000, People's Republic of China
e-mail: zhyz65@mail.ahnu.edu.cn

D. Feng · Y. Ling
Department of Chemistry, Wannan Medical College, Wuhu 241002, People's Republic of China

label of either antigen or antibody, or use the probe molecule in solution (e.g. ferricyanide or thionine). These methods may lead to the denaturation of the biomolecules. To overcome this drawback, label-free immunosensors have recently been reported via the changes of the current of signal molecule onto the interface of electrode [12–14]. For example, Ju and co-worker utilized thionine as signal molecule to develop a sensitive electrochemical CEA immunosensor [15]. Chen and his co-workers utilized gold nanoparticles-thionine-graphene composite for sensing interface and developed a sensitive electrochemical CEA immunosensor [16].

Among many redox mediators as signal molecule, Prussian Blue (PB) is a good materials and widely used in electrochemical sensors because of its advantages such as good redox properties, low cost [17, 18]. However, these sensors have a limit from leakage of PB from the electrode surface, leading to the stability of the PB film decreased [19, 20]. Therefore, it is considerable interest to search an effective and simple immobilized method of improving PB stability. For example, Li and co-workers have developed a sensitive electrochemical CEA immunosensor based on PB and carbon nanotubes composite for sensing interface [21]. Zhong and co-workers have reported on a novel electrochemical CEA immunosensor based on nanogold-enwrapped graphene nanocomposites as trace labels and PB nanoparticles acting as signal molecule [22]. Ou and co-workers have reported on a sensitive immunosensor based on PB, carbon nanotubes, Pt hybrid nanoparticles for sensing interface [23], Liu and co-worker also designed a sensitive amperometric immunosensor using PB and the organic–inorganic composite film as a sensing interface [24].

In this study, we designed a good approach to immobilize PB nanoparticles (PB-NPs) via alternate strategy of electrodeposition of PB and assembly of graphene and carbon nanotubes. Thus, the possibility of leakage of PB from the electrode surface was decreased and the stability of the biosensor was improved obviously. Multi-walled carbon nanotubes - graphene composites were employed to increase the electrode surface area and increase electron transfer rate of PB, gold nanoparticles (Au-NPs) was used for immobilizing the CEA antibody.

Experimental

Chemicals and reagents

Carcinoembryonic antigen (CEA), anti-CEA (antibody) and α-fetoprotein (AFP) was purchased from Biocell Biotech. Co. Ltd (Zhengzhou, China, http://chinabiocell.biogo.net) and stored in refrigerator at 4 °C. Poly (diallyldimethyammonium chloride) (PDDA) (200,000–350,000 MW) were purchased from Sigma Chemical Co (http://www.sigmaaldrich.com). Chitosan (MW=1,000,000, deacetylation degree 80–95 %) and Bovine serum albumin (BSA) were purchased from the Sinopharm Chemical Reagent Co., Ltd (Shanghai, China, http://www.reagent168.cn). Multi-walled carbon nanotubes with carboxylic acid groups (MWCNTs, with a diameter of about 20–30 nm and about length of 30 μm) were obtained from Chengdu Institute of Organic Chemistry, (Chinese Academy of Sciences http://www.timesnano.com). Reduced graphene oxide (rGO) was obtained from Sinocarbon Materials Technology Co., Ltd (Taiyuan, Shangxi, http://www.sinocarbon-cas.com). Chloroauric acid ($HAuCl_4 \cdot 4H_2O$), potassium ferricyanid ($K_3Fe(CN)_6$), potassium ferrocyanide ($K_4Fe(CN)_6 \cdot 3H_2O$), chloride hexahydrate ($FeCl_3 \cdot 6H_2O$) were purchased from the Shanghai Chemical Reagent Co., Ltd. (Shanghai, China, http://ccn.mofcom.gov.cn). Phosphate buffered saline (PBS) with various pH values were prepared by mixing the stock solutions of 0.025 $mol \cdot L^{-1}$ Na_2HPO_4, 0.025 $mol \cdot L^{-1}$ NaH_2PO_4 and 0.1 $mol \cdot L^{-1}$ KCl. The washing buffer was pH 6.0 PBS containing 0.05 % (W/V) Tween (PBST); Blocking solution was 1 % (W/W) BSA containing 0.05 % Tween. All solutions were prepared with twice-quartz-distilled water.

Apparatus

All electrochemical measurements were performed on a CHI 660A electrochemical workstation (Shanghai CH Instruments, Co. Ltd.). The three-electrode system consisted of a bare glassy carbon electrode (GCE) or the modified electrode as working electrode, a platinum wire as an auxiliary electrode, and an Ag/AgCl (3.0 $mol \cdot L^{-1}$ KCl) as reference electrode.

Scanning electron microscopy (SEM) (JEOLJSM-6700F, Hitachi, Japan) was used to obtain the morphologies of graphene, Au-NPs and PB-NPs. The size of the Au-NPs was measured with transmission electron microscope (TEM) (Hitachi-800).

Preparation of the PDDA-MWCNTs and rGO-MWCNTs composite materials

PDDA-MWCNTs were prepared according to the process described in literature [25]. Briefly, MWCNTs were firstly carboxylated by ultrasonic agitation for about 3 h in a mixture of sulfuric acid and nitric acid (3:1). Afterwards, the carboxylated MWCNTs were washed repeatedly with twice-quartz-distilled water till the solution was neutral. Finally, the carboxylated MWCNTs was dried at 100 °C.

Twenty milligrams carboxylated MWCNTs was dispersed into aqueous solution of 1.0 $mg \cdot mL^{-1}$ of the PDDA containing 0.5 $mol \cdot L^{-1}$ NaCl, and ultrasonic agitation for about 30 min to give a homogeneous suspension. Residual PDDA were removed by high-speed centrifugation and

rinsed with twice-quartz-distilled water for three times, thus, the PDDA-MWCNTs composite with positive charge was obtained.

rGO-MWCNTs composite materials was prepared according to the literature [26] with a little modification. Briefly, 40 mg rGO was added into 20 mL of 1.0 mg·mL^{-1} PDDA-MWCNTs dispersion with the rGO: MWCNTs weight ratios of 2:1. After then, the mixture was treated ultrasonically for 2 h until a homogenous dispersion was appeared. Subsequently, it was high-speed centrifugation and rinsed with water for three times. After the precipitate was dried at 60 °C for 12 h in the vacuum oven, it was again dispersed in twice-quartz-distilled water by treated ultrasonically to obtain rGO-MWCNTs stable solution of 1.0 mg·mL^{-1}.

Preparation of the gold nanoparticles

Au-NPs were prepared by reduction of $HAuCl_4 \cdot 4H_2O$ with sodium citrate [27]. Briefly, 50 mL solution of $HAuCl_4$ (0.01 %) was brought to boil, and 2.0 mL of 1 % sodium citrate solution was added, stirring vigorously. The mixture was stirred for 30 min and then cooled to room temperature while stirring. The diameter of the Au-NPs of about 15-nm was measured by TEM (Seen in supplementary Fig. S1). The Au-NPs obtained was stored in dark glass bottles at 4 °C for further use.

Fabrication of the electrochemical immunosensor

Before modification, the bare glassy carbon electrode (GCE) (3.0 mm in diameter, CH Instruments Inc) was treated according to our previous procedure [28]. Then, the electrode was dried in nitrogen atmosphere and for further use.

2.0 μL of rGO-MWCNTs composite was dropped onto the surface of pre-treated GCE and left to dry naturally at room temperature to form thin film. Afterwards, the electrode modified with rGO-MWCNTs was placed into electrolyte solution (2.5 mmol·L^{-1} $K_3Fe(CN)_6$ + 2.5 mmol·L^{-1} $FeCl_3$ + 0.1 mol·L^{-1} KCl) (pH=6.0), and cyclic potential scan for five cycles between 0.4 to −0.1 V at scan rate of 50 mV/s, thus, PB-NPs was deposited on the surface of the rGO-MWCNTs thin film.

2.0 μL of rGO-MWCNTs composite was again dropped onto the surface of PB-NPs film and cyclic potential scan for five cycles between 0.4 to −0.1 V in the same electrolyte solution, thus the second layer film of $(PB\text{-}NPs/rGO\text{-}MWCNTs)_2$ was obtained. Repeating the process above, the multi-layer films of $(PB\text{-}NPs/rGO\text{-}MWCNTs)_n$ could be obtained.

In order to avoid leakage of PB from electrode surface and improve the stability of the PB film, one good approach is to coat a substance with excellent biocompatibility on the surface of PB film [29]. According to this literature, we select 10.0 μL of chitosan (0.5 %) for dropping on the surface of the $(PB\text{-}NPs/rGO\text{-}MWCNTs)_n$ film. After drying naturally, the modified electrode was immersed in the Au-NPs solution for 4 h at 4 °C. Thus, the multi-layer films of Au-NPs/$(PB\text{-}NPs/rGO\text{-}MWCNTs)_n$ modified electrode was obtained.

Immobilization of anti-CEA was performed by dropping 10.0 μL of anti-CEA (200 μg·mL^{-1}) onto the surface of the Au-NPs/$(PB\text{-}NPs/rGO\text{-}MWCNTs)_n$ modified electrode and kept it in a refrigerator for 12 h. Thus, anti-CEA/Au-NPs/$(PB\text{-}NPs/rGO\text{-}MWCNTs)_n$ modified electrode was obtained. Finally, the modified electrode was incubated in blocking solution for 1 h at 37 °C to block possible remaining active sites and avoid the non-specific adsorption. When the modified electrode was not in use, it was stored in refrigerator.

Electrochemical detection of CEA

The antibody-antigen interaction was performed by immersing the immunosensor in various concentrations of CEA for 25 min. Then, the immunosensor was rinsed with PBST to remove the physically absorbed antigen. Differential pulse voltammetry (DPV) was employed to detect the changes of

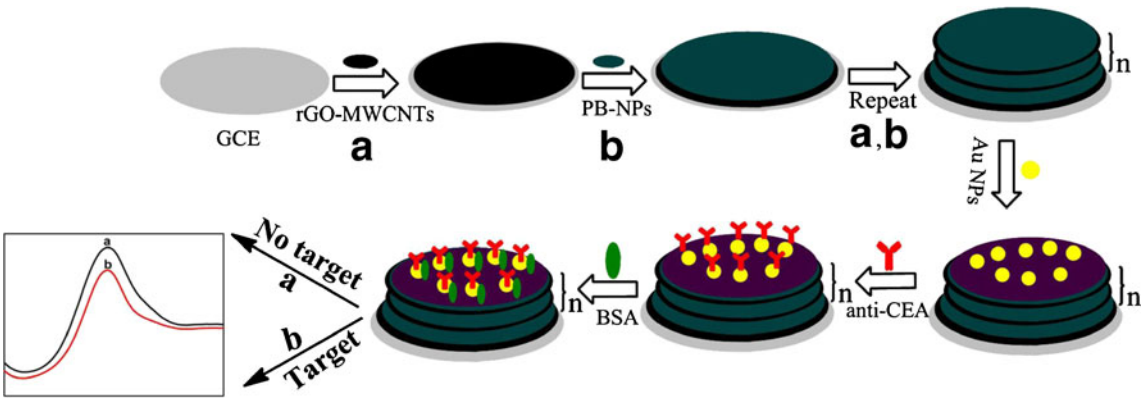

Scheme 1 Fabrication process of the electrochemical CEA immunosensor

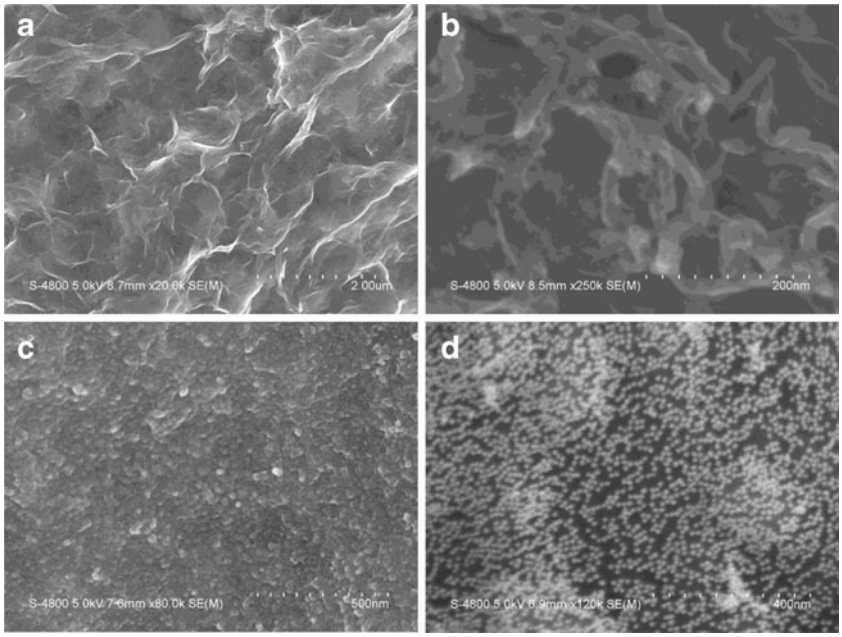

Fig. 1 SEM images of the different film **a** rGO, **b** rGO-MWCNTs, **c** PB-NPs/rGO-MWCNTs, **d** Au- NPs/(PB-NPs/rGO-MWCNTs)$_5$

the peak current of PB before and after the immunosensor recognized CEA in pH 6.0 PBS containing 0.1 mol·L^{-1} KCl. The concentration of CEA was quantified based on the relationship between the decline of the peak current and the concentration of CEA. The experiment parameters are listed as follows: potential range, −0.4 to 0.5 V; pulse amplitude, 0.05 V; sample width, 0.0167 s; pulse period, 0.2 s; quiet time: 2 s.

The fabrication process of the electrochemical CEA immunosensor is schematically illustrated in Scheme 1.

Results and discussion

Investigation of the assembled process of the immunosensor with SEM and electrochemical technique

SEM technique was used to investigate the assembled process of the immunosensor and their morphologies are shown in Fig. 1. It can be seen clearly that the rGO has crumpled structure (seen Fig. 1a), when the rGO was dispersed in MWCNTs solution, carbon nanotubes were clearly observed (seen Fig. 1b). When PB-NPs were electrodeposited on the surface of rGO-MWCNTs and Au-NPs were adsorbed on the surface of the PB-NPs/rGO-MWCNTs modified electrode. The global nanoparticles (PB-NPs and Au-NPs) were clearly observed and no aggregation occurred (seen in Fig. 1c and d), indicating the assembled process of the immunosensor was successful.

Figure 2 shows the cyclic voltammograms (CVs) of the different films of the (PB-NPs/rGO-MWCNTs)$_n$ in pH 6.0 PBS. A pair of redox peak of PB was observed with the peak potential of about 0.05 V and 0.10 V in the potential range of −0.4 to 0.8 V, respectively. As the number of layers increased, peak current (oxidative or reductive) increased clearly, which suggested that the electrochemical signal could be improved by the manner of multi-deposition and assembly. The peak current was linearly related to the numbers of the layers from 1 to 5. When layer further increased, the peak current decreased because the layers increased and the film became thicker, thus, the electron transfer ability of PB decreased. The highest current intensity of PB was obtained when the layer was five. Hence, we selected five layers film of the (PB-NPs/rGO-MWCNTs)$_5$ for this study.

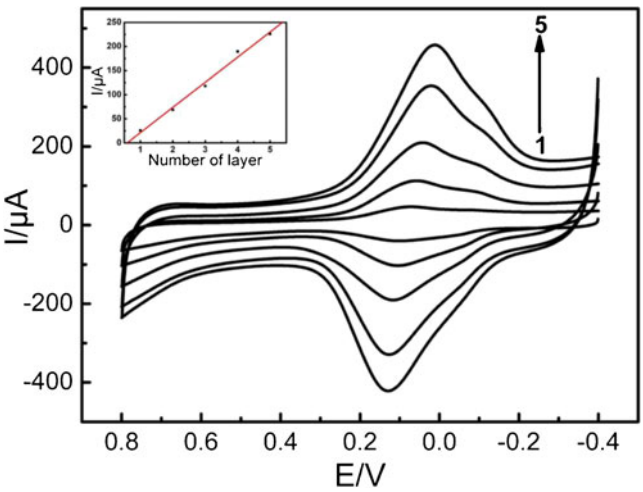

Fig. 2 CVs of the (PB-NPs/rGO-MWCNTs)$_n$ modified electrodes in pH 6.0 PBS containing 0.1 mol·L^{-1}KCl, where, n=1–5, scan rate: 50 mV·s^{-1}; *Inset*: Anodic peak current vs. number of layers

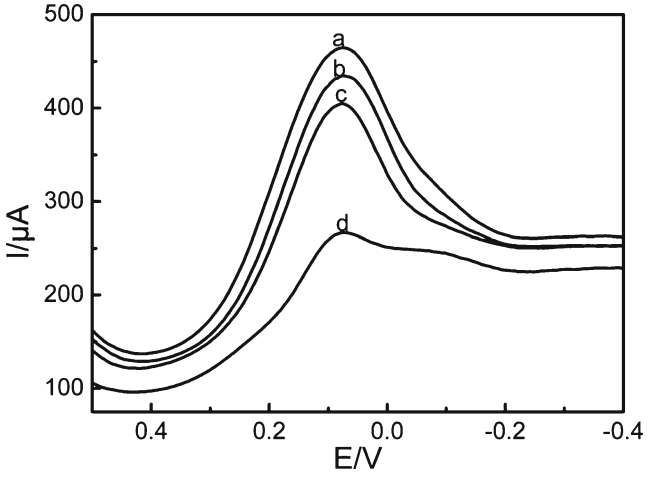

Fig. 3 DPVs of the immunosensor at different step in pH 6.0 PBS. (a) Au-NPs/(PB-NPs/rGO-MWCNTs)$_5$, (b) anti-CEA/Au-NPs/(PB-NPs/rGO-MWCNTs)$_5$ (c) BSA/anti-CEA/Au-NPs/(PB-NPs/rGO-MWCNTs)$_5$ film modified electrode, (d) the (c) in presence of 10 ng·mL^{-1} CEA antigen

The principal of the electrochemical immunosensor

The principal of the immuosensor detect CEA are based on the relationship between the decline of the peak current of the immobilized PB-NPs and the concentration of CEA.

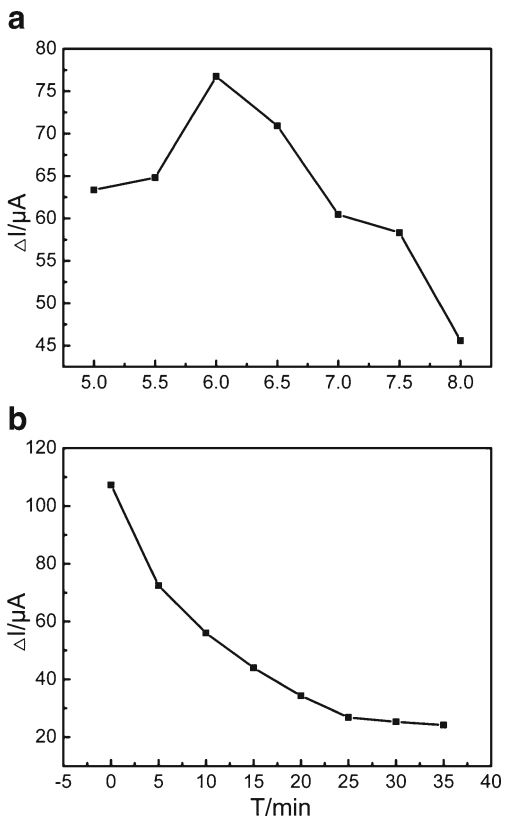

Fig. 4 Effect of the pH (**a**) and the incubation time (**b**) on the signal of the immunosensor C $_{CEA}$=0.6 ng·mL^{-1}

Figure 3 shows the differential voltammograms (DPVs) of the immunosensor at different step. A greater peak current was observed at the Au-NPs/(PB-NPs/rGO-MWCNTs)$_5$ films modified electrode (curve a), and the peak current decreased clearly when the anti-CEA was immobilized on the surface of the Au-NPs/(PB-NPs/rGO-MWCNTs)$_5$ films due to the anti-CEA hindered the electron transfer of PB-NPs (curve b); When BSA was immobilized onto the surface of the modified electrode, a further decrease of the peak current was observed because BSA is a larger biomolecule and further block the electron transfer of PB (curve c). In the presence of CEA, the peak current continuously decreased due to the formation of the antigen-antibody immunocomplex blocked the tunnel for mass and electron transfer of PB (curve d). As the CEA concentration increased, the peak current was further decreased. Therefore, the CEA concentration can be obtained based on the relationship between decline of peak current and CEA concentration.

Optimization of experimental conditions

In this study, in order to obtain good performance of immunosensor, some experiment parameters were

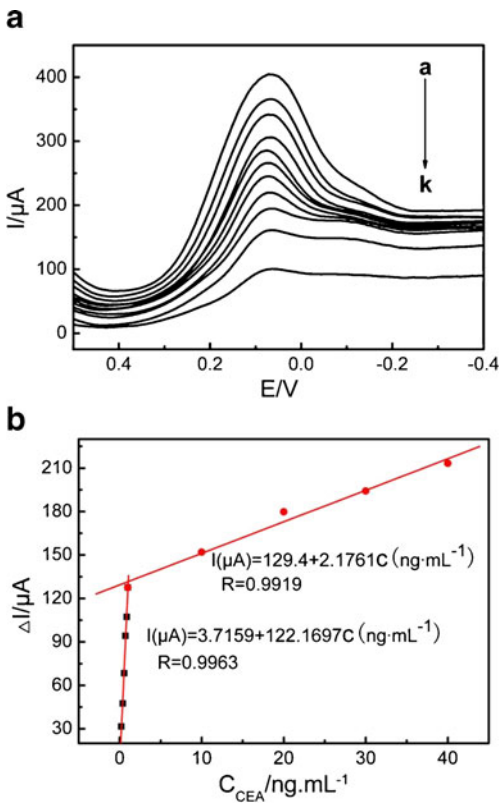

Fig. 5 **a** DPVs of the immunosensors at different concentrations of CEA (from a to k: 0; 0.2; 0.385; 0.556; 0.715; 0.860; 1.0; 10; 20; 30 and 40 ng·mL^{-1}). **b** Calibration plots of the peak current (ΔI) vs. antigen concentration

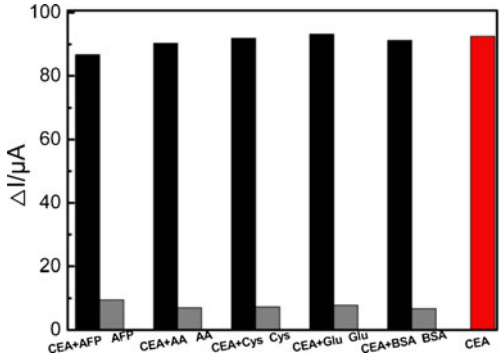

Fig. 6 The decline of the peak current of the immunosensor in the presence of 10 ng·mL^{-1} of CEA (*red bar*), 50 ng·mL^{-1} of other interfere substances (*grey bar*) and mixtures of 10 ng·mL^{-1} of CEA and 50 ng·mL^{-1} interfere substances (*black bar*)

investigated (such as pH, incubation time). Figure 4a shows the peak currents of the immunosensor at different pH (from 5.0 to 8.0), it was observed clearly that the peak currents of the immunosensor was increased as pH value increased from 5.0 to 6.0 and decreased since then. The reason is that the PB is easily decomposed in alkaline conditions and stability of the film is decreased.

Figure 4b shows the peak currents response of the immunosensor in different the incubation times (0–35 min). It was observed clearly that the peak current decreased rapidly as increasing incubation time from 0 to 25 min. After that, it decreased slowly and almost kept a constant, indicating the immunoreaction of antigen-antibody was finished. Therefore, 25 min was used for the incubation time in this study. In this work, temperature of the immunoreaction is chosen at 37 °C because higher temperature may damage the activity of the antibody and antigen.

Analytical performance

The analytical performance of this CEA immunosensor was evaluated using the immunosensor to detect different concentration of CEA under the optimal conditions and the results are shown in Fig. 5a. It can be observed that the peak current of PB decreased as the concentration of CEA increased, and the decline of the peak current was linearly related to the concentration of CEA in the two ranges of (0.2–1.0, 1.0–40 ng·mL^{-1}) with a detection limit of 60 pg·L^{-1} (at S/N=3) (seen in Fig. 5b). The linear regression equation was $\Delta I=3.7159+122.1697C$ (unit of C is ng·mL^{-1}, unit of I is μA) (0.2–1.0 ng·mL^{-1}) and $\Delta I=129.4+2.1761C$ (unit of C is ng·mL^{-1}, unit of I is μA) (1.0–40 ng·mL^{-1}), and regression coefficient was 0.9963 and 0.9919, respectively. Because of the threshold values of CEA in normal human serum is 5.0 ng·mL^{-1}. So, the electrochemical immunosensors could completely meet the requirements of clinical analysis.

Compared with similar work reported, the immunosensor has wider linear range over these immunosensors including anti-CEA/Au-NPs/CS-MWCNTs (0.50–25.0 ng·mL^{-1}) [30], poly-OAP/CEAAb–Au-NPs/Au (0.5–20 ng·mL^{-1}) [31], CEA/nanogold/MPTS/Fe_3O_4-CPE (1.0–55 ng·mL^{-1}) [32]. It was mainly attributed to the more mount of the anti-CEA immobilization at the surface of the Au-NPs/(PB-NPs/rGO-MWCNTs)$_5$ film. At the same time, rGO-MWCNTs nanocomposite improves the electron transfer ability of PB. The linear range was narrower than that of the immunosensor of thionine and ferrocene as distinguishable signal tags (0.01–50 ng·mL^{-1}) [33]. However, the immunosensor need labeled antibody or antigen with thionine or ferrocene, the fabrication process is more complex.

Selectivity of the immunosensor

In this study, we investigated the effect of various substances on the detection of CEA by recording the change of peak current in the absence and presence of interferes (such as AFP, AA, glucose, L-cysteine), and the results are shown with histograms in Fig. 6. It was observed that the immunosensor showed an almost neglectable response to interferes (50 ng·mL^{-1}) compared with that of the CEA (10 ng·mL^{-1}). When the immunosensor detected the mixture of 10 ng·mL^{-1} of CEA and 50 ng·mL^{-1} of another interferes, the response signal of the mixture changed a little in contrast to CEA alone, which indicated that the biosensor possess excellent selectivity.

Reproducibility, stability of the immunosensor

The reproducibility of the immunosensor was investigated by detecting three different concentrations of CEA (0.70 ng·mL^{-1}, 1.0 ng·mL^{-1}, 10 ng·mL^{-1}) using identical immunosensor. The peak current is 91.26, 93.49, 89.60, 85.60, 82.63 μA for 0.70 ng·mL^{-1}, 118.0, 115.7, 112.8,

Table 1 Analytical results in serum samples

Serum Sample	1	2	3	4	5
This method [a] (ng·mL^{-1})	1.00±0.13	7.62±0.25	8.56±0.2	9.12±0.31	10.81±0.7
ELISA [a] (ng·mL^{-1})	1.06±0.17	7.06±0.28	9.07±0.13	8.73±0.32	11.25±0.5
Relative deviation (%)	−5.67	7.36	−5.62	+4.49	−3.91

[a]Mean value ± SD of five measurements

122.5, 110.2 μA for 1.0 ng·mL^{-1} and 151.2, 149.6 147.8, 158.8, 149.0 μA for 10 ng·mL^{-1}. The coefficients of variation of the intra-assay was 4.37 %, 4.74 % and 4.38 %, respectively, whereas the inter-assay was investigated using five immunosensors to detect three different concentrations of CEA(0.70 ng·mL^{-1}, 1.0 ng·mL^{-1}, 10 ng·mL^{-1}), the coefficients of variation were 6.98 %, 5.40 % and 5.22 %, respectively. Thus, the precision and reproducibility of the immunoassay were satisfied.

The stability of the immunosensor was investigated by CV techniques and record the peak current, the RSD was 4.0 % after 40 cyclic scans. The long - time stability of the immunosensor was investigated by testing once time every day and the peak current also kept a constant during 3 weeks.

Evaluation of clinical specimens with the immunosensor

In order to examine the applicability of the immunosensor for practical analyses, the recovery experiments were performed by standard addition methods. The standard samples of CEA were dissolved in the healthy human serum (the concentrations range of the CEA is within 0.2 to 40 ng·mL^{-1}) and detected the CEA in serum. The recovery obtained is within 96.7–110 %, indicating the method is suitable for serum sample analysis (seen in Table S1).

The feasibility of the immunoassay for clinical applications was investigated by analyzing several real samples in comparison with the commercial enzyme-linked immunosorbent assay (ELISA) method. Five serum specimens containing CEA were from the clinical laboratory of the Yiji Shan Hospital (Wuhu, China). These results are shown in Table 1. It can be seen that the value obtained are in agreement with that of the ELISA, indicting the immunosensor can be applied to serum analysis.

Conclusions

In this study, we reported a sensitive label-free electrochemical immunosensor for the detection of CEA via the alternate strategy of electrodeposition and self-assembly technique. The immunosensor present two features: First, the multilayer films of the $(PB\text{-}NPs/rGO\text{-}MWCNTs)_n$ has higher stability and provides more amount of anti-CEA immobilization. Second, the rGO-MWCNTs improve the electron transfer ability of PB. Therefore, the immunosensor exhibited higher sensitivity, good stability.

Acknowledgments This work was supported by the National Natural Science Foundation of China (No. 20675002) and the Young Program of Wannan Medical College (No.WK201210 and 201120)

References

1. Hernandez L, Espasa A, Fernandez C, Candela A, Martin C, Romero S (2002) CEA and CA 549 in serum and pleural fluid of patients with pleural effusion. Lung Cancer 36:83–89
2. Jezersek B, Cervek J, Rudolf Z, Novakovic S (1996) Linical evaluation of potential usefulness of CEA, CA 15–3, and MCA in follow-up fo breast cancer patients. Cancer Lett 110:137–144
3. Chandra KD, Sandeep KV, Feidhlim TO, Brian O, Brian DM, Richard O (2010) Development of a high sensitivity rapid sandwich ELISA procedure and its comparison with the conventional approach. Anal Chem 82:7049–7052
4. Rebe RS, Bremer MG, Haasnoot W, Norde W (2009) Label-free and multiplex detection of antibiotic residues in milk using imaging surface plasmon resonance-based immunosensor. Anal Chem 81:7743–7749
5. Xu SJ, Liu Y, Wang TH, Li JH (2011) Positive potential operation of a cathodic electrogenerated chemiluminescence immunosensor based on luminol and graphene for cancer biomarker detection. Anal Chem 83:3817–3823
6. Song ZJ, Yuan R, Chai YQ, Yin B, Fu P, Wang JF (2010) Multilayer structured amperometric immunosensor based on gold nanoparticles and prussian blue nanoparticles/nanocomposite functionalized interface. Electrochim Acta 55:1778–1784
7. Mani V, Chikkaveeraiah B, Patel V, Gutkind J, Rusling J (2009) Ultrasensitive immunosensor for cancer biomarker proteins using gold nanoparticles film electrodes and multienzyme-particle amplification. ACS Nano 3:584–794
8. Laboria N, Fragoso A, Kemmner W, Latta D, Nilsson O, Botero M, Drese K, Sullivan O (2010) Amperometric immunosensor for carcioembryonic antigen in colon cancer samples based on monolayers of dendritic bipodal scaffolds. Anal Chem 82:1712–1719
9. Tang DP, Su BL, Tang J, Ren JJ, Chen GN (2010) Nanoparticle-based sandwich electrochemical immunoassay for carbohydrate antigen 125 with signal enhancement using enzyme-coated nanometer-sized enzyme-doped silica beads. Anal Chem 82:1527–1534
10. Yuan Y, Yuan R, Chai YQ, Zhuo Y, Shi Y, He X, Miao X (2007) A reagentless amperometric immunosensor for α-fetoprotein based on gold nanoparticles/TiO_2 colloid/Prussian blue modified platinum electrode. Electroanalysis 19:1402–1410
11. Tian JN, Huang JL, Zhao YC, Zhao SL (2012) Electrochemical immunosensor for prostate-specific antigen using a glassy carbon electrode modified with a nanocomposite containing gold nanoparticles supported with starch-functionalized multi-walled carbon nanotubes. Microchim Acta 178:81–88
12. Gao X, Zhang YM, Chen H, Chen ZH, Lin XF (2011) Amperometric immunosensor for carcinoembryonic antigen detection with carbon nanotube-based film decorated with gold nanoclusters. Anal Biochem 414:70–76
13. Wang GF, Zhang G, Huang H, Wang L (2011) Graphene-Prussian blue/gold nanoparticles based electrochemical immunoassay of carcinoembryonic antigen. Anal Methods 3:2082–2087
14. Mi Q, Wang ZW, Chai CY, Zhang J, Zhao B, Chen CY (2011) Multilayer structured immunosensor based on a glassy carbon electrode modified with multi-wall carbon nanotubes, polythionine, and gold nanoparticles. Microchim Acta 173:459–467
15. Wu J, Tang JH, Dai Z, Yan F, Ju HX, Murr NE (2006) A disposable electrochemical immunosensor for flow injection immunoassay of carcinoembryonic antigen. Biosens Bioelectron 22:102–108
16. Kong FY, Xu MT, Xu JJ, Chen HY (2011) A novel label-free electrochemical immunosensor for carcinoembryonic antigen based on gold nanoparticles-thionine-reduced graphene oxide nanocomposite film modified glassy carbon electrode. Talanta 85:2620–2625

17. Lv P, Min LG, Yuan R, Chai YQ, Chen SH (2010) A novel immunosensor for carcinoembryonic antigen based on poly(diallyldimethylammonium chloride) protected Prussian blue nanoparticles and double-layer nanometer-sized gold particles. Microchim Acta 171:297–304
18. Zhao H, Yuan Y, Adeloju S, Wallace G (2002) Study on the formation of the Prussian blue films on the polypyrrole surface as a potential mediator system for biosensing applications. Anal Chim Acta 472:113–121
19. Jiang W, Yuan R, Chai YQ, Yin B (2010) Amperometric immunosensor based on carbon nanotubes/Prussian blue/nanogold-modified electrode for determination of α-fetoprotein. Anal Biochem 407:65–71
20. Haghighi B, Varma S, Alizadeh FM, Yigzaw Y, Gorton L (2004) Prussian blue modified glassy carbon electrodes-study on operational stability and its application as a sucrose biosensor. Talanta 64:3–12
21. Li Z, Chen J, Li W, Chen K, Xie L, Yao S (2007) Improved electrochemical properties of prussian blue by multi-walled carbon nanotubes. J Electroanal Chem 603:59–65
22. Zhong ZY, Wu W, Wang D, Wang D, Shan JL, Qing Y, Zhang ZM (2010) Nanogold-enwrapped graphene nanocomposites as trace labels for sensitivity enhancement of electrochemical immunosensors in clinical immunoassays: carcinoembryonic antigen as a model. Biosens Bioelectron 25:2379–2383
23. Ou CF, Chen SH, Yuan R, Chai YQ, Zhong X (2008) Layer-by-layer self-assembled multilayer films of multi-walled carbon nanotubes and platinum-prussian blue hybrid nanoparticles for the fabrication of amperometric immunosensor. J Electroanal Chem 624:287–292
24. Liu ZY, Yuan R, Chai YQ, Zhuo Y, Hong CL, Yang X (2008) Highly sensitive, reagentless amperometric immunosensor based on a novel redox-active organic–inorganic composite film. Sensors Actuators B 134:625–631
25. Cui RJ, Huang HP, Yin ZZ, Gao D, Zhu JJ (2008) Horseradish peroxidase-functionalized gold nanoparticle label for amplified immunoanalysis based on gold nanoparticles/carbon nanotubes hybrids modified biosensor. Biosens Bioelectron 23:1666–1673
26. Chen SQ, Yeoh WK, Liu Q, Wang GX (2012) Chemical-free synthesis of graphene–carbon nanotube hybrid materials for reversible lithium storage in lithium-ion ban. Carbon 50:4557–4565
27. Enustum B, Turkevich J (1963) Coagulation of colloidal gold. J Am Chem Soc 85:3317–3328
28. Zhang YZ, Huang L (2012) Label-free electrochemical DNA biosensor based on a glassy carbon electrode modified with gold nanoparticles, polythionine, and graphene. Microchim Acta 176:463–470
29. Song ZJ, Yuan R, Chai YQ, Wang JF, Che X (2010) Dual amplification strategy for the fabrication of highly sensitive amperometric immunosensor based on nanocomposite functionalized interface. Sensors Actuators B 145:817–825
30. Huang KJ, Niu DJ, Xie WZ, Wang W (2010) A disposable electrochemical immunosensor for carcinoembryonic antigen based on nano-Au/multi-walled carbon nanotubes-chitosans nanocomposite film modified glassy carbon electrode. Anal Chim Acta 659:102–108
31. Tang H, Chen JH, Nie LH, Kuang YF, Yao ZS (2007) A label-free electrochemical immunoassay for carcinoembryonic antigen based on gold nanoparticles and nonconductive polymer film. Biosens Bioelectron 22:1061–1067
32. Dian YT, Bi YX (2008) Electrochemical immunosensor and biochemical analysis for carcinoembryonic antigen in clinical diagnosis. Microchim Acta 163:41–48
33. Lai WQ, Zhang JY, Tang J, Chen GN, Tang DP (2012) One-step electrochemical immunosensing for simultaneous detection of two biomarkers using thionine and ferrocene as distinguishable signals tags. Microchim Acta 178:357–365